

# MoboTSP: Solving the Task Sequencing Problem for Mobile Manipulators

Nicholas Adrian and Quang-Cuong Pham

**Abstract**—We introduce a new approach to tackle the mobile manipulator task sequencing problem. We leverage computational geometry, graph theory and combinatorial optimization to yield a principled method to segment the task-space targets into reachable clusters, analytically determine base pose for each cluster, and find task sequences that minimize the number of base movements and robot execution time. By clustering targets first and by doing so from first principles, our solution is more general and computationally efficient when compared to existing methods.

## I. INTRODUCTION

A mobile manipulator consists of a manipulator (e.g. a robotic arm) mounted unto a mobile base. The combined system extends the workspace of a fixed-based manipulator [1] [2] [3].

A frequent task for a mobile manipulator is to visit a set of ordered or unordered targets scattered around the workspace: think for example of drilling multiple holes on aircraft fuselages or on curved housing walls (Fig. 1). Another example is motivated by mobile 3D-printing of large workpieces [4].

For fixed-based manipulators, finding the optimal sequence of targets and the corresponding Inverse Kinematics (IK) solutions is known as the Robotic Task Sequencing Problem (RTSP) see [5] for a recent review. Compared to fixed-base manipulators, solving RTSP for mobile manipulators comes with extra complexities due to the distribution of task space targets that spans beyond the reachable workspace of a fixed-base manipulator.

One solution may consist of segmenting *a priori* the targets into what we call *workspace clusters*. Each *workspace cluster* would contain *workspace targets* that can be reached by a corresponding *workspace base pose*. However, when there is no evident of *a priori* spatial clusters, this hierarchical approach will likely result in suboptimal solutions.

Here we introduce a new approach to tackle mobile manipulator task sequencing problem. We leverage computational geometry, graph theory and combinatorial optimization to yield a principled method to segment the task point targets into reachable clusters, analytically determine base pose for each cluster, and find task sequences that minimize the number of base movements and robot execution time.

Note that the minimization of the number of base movements has the highest priority, as such movements are the largest source of localization errors (as compared to the kinematic errors of a fixed-base manipulator).

The authors are with the HP-NTU Digital Manufacturing Corporate Lab and School of Mechanical and Aerospace Engineering, Nanyang Technological University, Singapore. Email: nicholasadr@ntu.edu.sg

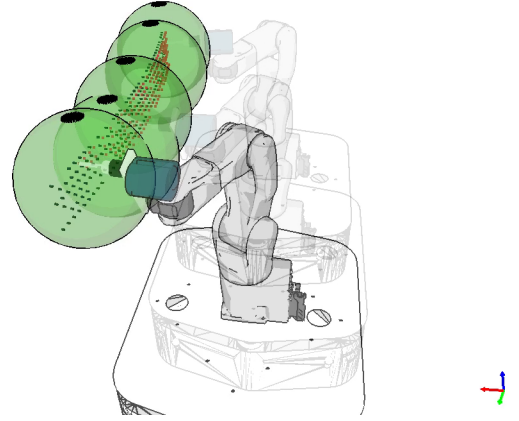


Fig. 1: Example of a mobile manipulator consisting of a Denso VS60 robot arm mounted on a Clearpath Ridgeback mobile base. The task is to perform drilling on a set of targets on a curved surface. There is no *a priori* constraint on the target cluster or sequence.

Our contributions are as follows:

- A method to find a set of balls within the manipulator's workspace, such that all the points contained in the balls are reachable from all the directions of a given cone. This is useful in both fixed-base and mobile manipulator cases;
- A method to cluster targets by covering by balls and to obtain the respective base pose in each cluster;
- A task sequencing algorithm for mobile manipulator, minimizing the number of base movements and the manipulator trajectory time within and between *workspace clusters*.

The remainder of the paper is organized as follows. In Section II, we review related works in mobile manipulator task sequencing. In Section III, we introduce the overall pipeline. In Section IV, we present the detailed calculations of the set of balls. In Section V, we introduce our method to cluster the targets into separate workspaces, followed by task sequencing algorithm in Section VI. We present the simulation results in Section VII. Finally, in Section VIII, we conclude and sketch directions for future work.

## II. LITERATURE REVIEW

To start with, we look at some works on finding robot placement. In [6], reachability map is introduced as a 3D workspace representation that represents the reachability probability of points in task space. The reachability map is

used in [7] to find robot placement for a constrained linear trajectory. The work is extended in [8] to 3D trajectory. In [9], extended manipulability measure as quality index is used as precomputed workspace representation instead of reachability. Robot placement can also be found using Inverse Reachability Distribution [10].

Several works on RTSP have been attempted but they are mostly limited to fixed-base manipulator. In [11], Genetic Algorithm (GA) is employed on 3-DOF and 6-DOF robots with multiple IK solutions per target. They reported 1800 seconds CPU time for 50 task points. This work was extended in [12] to include base placement of the robot. No computational details were provided for varying number of task points or base permutations per task point. In [13], the author considered 50 targets with five configurations each and the solution was found in 9621.64 seconds. The fastest solution for fixed-based manipulator RTSP, to our best understanding, is found in [5]. A fast near-optimal solution was found using a three-step algorithm exploiting both task and configuration space. In their experiment, they visited 245 targets with an average of 28.5 configurations per target and the solution was found in 10 seconds with 60 seconds execution time. For the case of mobile manipulator, a search on 10-DOF configuration space is done as part of Genetic Algorithm-based optimization to minimize overall configurations displacement in [1].

In [2], a relatively similar problem of part-supply pick and place is presented where the robot had to pick parts from multiple tray locations. Given  $m$  number of trays containing  $n$  number of objects with  $o$  number of possible grasping poses each,  $m \times n \times o$  IK queries would be required. Objects are also pre-clustered into trays which reduce the number of base regions to consider. However, such target clustering might not be available or easily defined in other cases such as when continuous target distribution is involved.

In [3], the mobile manipulator's end-effector has to follow a continuous path trajectory. To deal with inaccurate base locomotion, the author used manipulability performance function to find minimum base stopping positions that will allow the robot to follow discretized points on the path trajectory. However this method requires the discretized target points to be pre-sequenced.

Compared to other methods, our approach exploits the often overlooked strategy of clustering targets first. This allows us to have a fast and computationally efficient solution. In Section VII, we show that we clustered 183 targets in 0.104 seconds. To our best understanding, no other solutions have been able to do so in a systematic way while also providing an analytical solution for finding base poses that can reach all the targets in each cluster.

### III. PIPELINE

We assume that the targets' positions  $\mathbf{x}_k = [x_x^k, x_y^k, x_z^k]$ ,  $k \in [1, n]$  of  $\mathbf{X} \in \mathbb{R}^{n \times 3}$  and their respective drilling direction vectors  $\mathbf{R} \in \mathbb{R}^{n \times 3}$  are provided for all  $n$  targets.

- 1)  $\mathbf{X}$  is segmented into  $c$  clusters of  $\mathbf{X}_i$  for  $i \in [1, c]$ .  $\mathbf{X}_i$  is guaranteed to be geometrically covered by a *ball* of center position  $\mathbf{c}_i$  and diameter  $d$ . Refer to Figure 2a.
- 2) Each *ball* centered at  $\mathbf{c}_i$  is matched with  $\mathcal{B}(\mathbf{c}_i) \subseteq \mathcal{B}$  where  $\mathcal{B}$  is a pre-calculated set of *balls* with the same diameter  $d$  relative to the robot's frame. Through this matching process, we immediately obtain the robot's base pose  $\mathbf{T}_{base}^i$  to visit the target cluster  $\mathbf{X}_i$ . The details on how  $\mathcal{B}$  is obtained is included in Section IV. Refer to Figure 2b.
- 3) Base tour that minimizes base pose distance in *task-space* between  $\mathbf{X}_i$  is calculated.
- 4) Manipulator tour is calculated that respects the base tour.
- 5) Collision-free trajectory is calculated based on obtained base and manipulator tour.

### IV. REACHABLE SET OF BALLS

Note that  $\mathbf{c}_i$ 's center coordinate can vary in x,y,z axes. Thus, we need to find a set of balls  $\mathcal{B}$  of varying center heights to account for the variation during matching. Variation in  $\mathbf{c}_i$ 's coordinate in xy-plane can be easily handled by the base locomotion.

We pre-calculate a set of *balls*  $\mathcal{B}$  with diameter  $d$  relative to the robot's frame such that the balls' centers form a continuous straight line in 3D, close-bounded by the highest and lowest balls.

Let  $\mathcal{P} \in \mathbb{R}^3$  be the continuous set of all points within a closed ball of center coordinate  $\mathbf{b}$  and diameter  $d$ :

$$\mathcal{P}(\mathbf{b}) = \{\mathbf{p} : \|\mathbf{p} - \mathbf{b}\| \leq (d/2)^2\}$$

As mentioned in Section III, each  $\mathbf{X}_i$  ball cluster centered at  $\mathbf{c}_i$  is matched with a ball  $\mathcal{B}(\mathbf{c}_i) \subseteq \mathcal{B}$ . Any distribution of targets in  $\mathbf{X}_i$  matched with  $\mathcal{B}(\mathbf{c}_i)$  is guaranteed to be reachable from any directions in  $\mathbf{R}$  if all points in  $\mathcal{P}(\mathcal{B}(\mathbf{c}_i))$  is reachable from all directions in  $\mathbf{R}$ . Since it is impossible to check for every point in the continuous space of  $\mathcal{P}(\mathcal{B}(\mathbf{c}_i))$  and  $\mathbf{R}$ , we apply an approximation condition: Every point in the discretized  $\mathcal{P}(\mathcal{B}(\mathbf{c}_i))$  must be reachable from the directions bounding  $\mathbf{R}$ .

To do so, we construct a *focused kinematic reachability* (fkr) database which involves discretizing the Cartesian workspace into 3D voxels. For each voxel position, we perform Inverse Kinematics (IK) to obtain a set of IK solutions for each direction in  $\mathbf{R}_{ext} \subseteq \mathbf{R}$  where  $\mathbf{R}_{ext}$  contains the bounding directions for  $\mathbf{R}$ . All voxels containing IK solutions for all directions in  $\mathbf{R}_{ext}$  are then marked and saved as  $\mathbf{V}_{fkr}$ .

Given that  $\mathbf{V}_{fkr}$  represents the discretized volume that is reachable from the directions bounding  $\mathbf{R}$ , we can now proceed to find the set of balls  $\mathcal{B}$  within the  $\mathbf{V}_{fkr}$  that fulfills the condition above. To make the problem tractable, we can solve this with simple linear programming if we can obtain a maximal convex representation of  $\mathbf{V}_{fkr}$ . Finding the largest convex subset is often known as finding the *Maximal Area/Surface Convex Subset* (MACS), *potato-peeling* or *convex skull* problem. More specifically, we are

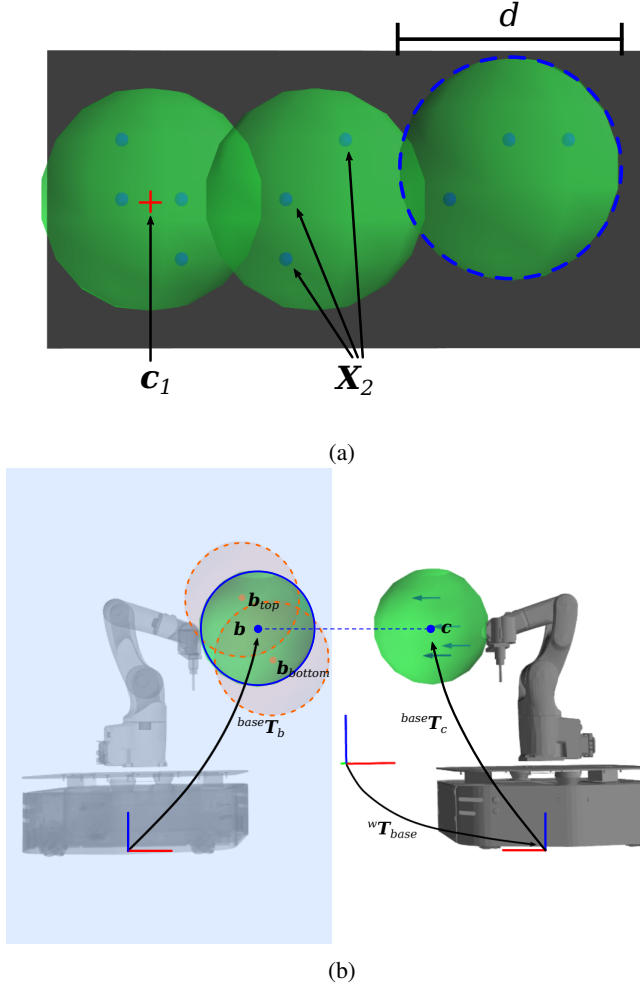


Fig. 2: (a) Illustration of how  $\mathbf{X}$  is segmented into  $c = 3$  clusters of  $\mathbf{X}_1$ ,  $\mathbf{X}_2$ , and  $\mathbf{X}_3$  with equal diameter  $d$ . The red cross represents the center coordinate for  $\mathbf{X}_1$  cluster. (b) Left: The set of balls  $\mathcal{B}$  is defined by the center coordinates  $\mathbf{b}_{\text{top}}$  and  $\mathbf{b}_{\text{bottom}}$  shown in orange dots. The outer shapes of the top and bottom balls of diameter  $d$  are displayed in dashed orange circle. Right: Target cluster  $\mathbf{X}_i$  is covered by a ball centered at  $\mathbf{c}_i$  with diameter  $d$ . Matching: Ball centered at  $\mathbf{c}_i$  can be matched with the respective ball  $\mathcal{B}(\mathbf{c}_i) \subseteq \mathcal{B}$  centered at  $\mathbf{b}_i$  such that  ${}^{\text{base}}\mathbf{T}_{\mathbf{b}_i} = {}^{\text{base}}\mathbf{T}_{\mathbf{c}_i}$ .

dealing with the *digital* [14] [15] variation given  $\mathbf{V}_{\text{fkr}}$  is in integer coordinates. In this paper, we implemented a heuristic for 3D *digital potato-peeling* from [14] to obtain a MACS approximation  $\mathbf{M}_{\text{fkr}}$ . Refer to Figure 3 for an example of our MACS finding algorithm implementation.

Finally, we find the ball set  $\mathcal{B}$  that lies within  $\mathbf{M}_{\text{fkr}}$  via linear programming [16]. By convexity, we can define  $\mathcal{B}$  by simply finding two balls on the extreme ends with center coordinates  $\mathbf{b}_{\text{top}} = [b_x^t, b_y^t, b_z^t]$  and  $\mathbf{b}_{\text{bottom}} = [b_x^b, b_y^b, b_z^b]$  respectively where  $b_z^t = \max(\text{height}(x^i))$  and  $b_z^b = \min(\text{height}(x^i))$ . The linear program has to fulfill the following inequalities and equalities constraints which are

visualized in Figure 4:

$$\begin{aligned} & \min_x \mathbf{e}^T \mathbf{a} \\ & \text{such that } \mathbf{A}_{\text{m fkr}} \mathbf{a} \leq \mathbf{b}_{\text{m fkr}} \\ & [-1, 0, 0, 0, 0, 0, 1]^T \mathbf{a} \leq x_{\text{offset}} \\ & [0, 0, 0, -1, 0, 0, 1]^T \mathbf{a} \leq x_{\text{offset}} \\ & [0, 0, -1, 0, 0, 0, 1]^T \mathbf{a} \leq z_{\text{offset}} \\ & [0, 0, 0, 0, 0, -1, 1]^T \mathbf{a} \leq z_{\text{offset}} \\ & [0, 0, 1, 0, 0, 0, 0]^T \mathbf{a} = \min(\text{height}(x^i)) \\ & [0, 0, 0, 0, 0, 1, 0]^T \mathbf{a} = \max(\text{height}(x^i)) \end{aligned}$$

$$\begin{aligned} & \text{where } \mathbf{e}^T = [0, 0, 0, 0, 0, 0, -1] \\ & \mathbf{a} = [b_x^b, b_y^b, b_z^b, b_x^t, b_y^t, b_z^t, d/2] \\ & \mathbf{A}_{\text{m fkr}} = \mathbf{M}_{\text{fkr}} \text{ plane coefficients} \\ & \mathbf{b}_{\text{m fkr}} = \mathbf{M}_{\text{fkr}} \text{ plane offsets} \\ & x_{\text{offset}} = \text{X-axis collision plane} \\ & z_{\text{offset}} = \text{Z-axis collision plane} \end{aligned}$$

## V. WORKSPACE CLUSTERING

The goal here is to segment  $\mathbf{X}$  into  $\mathbf{X}_i$  clusters and obtain the base pose  $\mathbf{T}_{\text{base}}^i$  that can reach all the targets in  $\mathbf{X}_i$ .

We do this by clustering  $\mathbf{X}$  in 3D space and ensuring that each  $\mathbf{X}_i$  is contained within a ball centered at  $\mathbf{c}_i$  of diameter  $d$  which is then matched with the corresponding ball  $\mathcal{B}(\mathbf{c}_i) \subseteq \mathcal{B}$ .

We formulate the problem of 3D points covering with balls as partitioning graph by cliques or *clique covering*. We form the undirected graph  $\mathcal{G}$  by connecting two nodes (targets) if the Euclidean distance between them is less or equal to  $\delta$  such that the clique can be covered by ball of diameter  $d$ . Clustering by clique in  $\mathcal{G}$  is similar to covering by independent set in the complement graph  $\bar{\mathcal{G}}$  which is often referred to as the *graph-coloring* problem. *Graph-coloring* problem is NP-complete but several heuristics exist [17] [18] [19]. In this paper we implemented greedy coloring of connected sequential breadth-first search variant [17] as it results in minimum average number of clusters based on our experiment.

The calculation for  $\delta$  is presented here. Let  $e$  be the center of a circle with radius  $\delta$  and  $f$  is a point on the circle's circumference as illustrated in Figure 5. Points  $e$  and  $f$  are of distance  $\delta$  and hence would be connected by an edge if they are nodes in the Graph  $\mathcal{G}$ . Point  $g$  is the intersection point between two circles centered at  $e$  and  $f$  of similar radius  $\delta$  and the three points form a clique. Circle  $O$  is smallest circle that circumscribes points  $e, f$ , and  $g$ . It is clear that any maximal clique that contains the three points will be contained inside  $O$  with diameter  $d$ . As this theorem extends to 3D, we can then find the relation between ball diameter  $d$  and maximum edge length  $\delta$  by solving for the circumradius

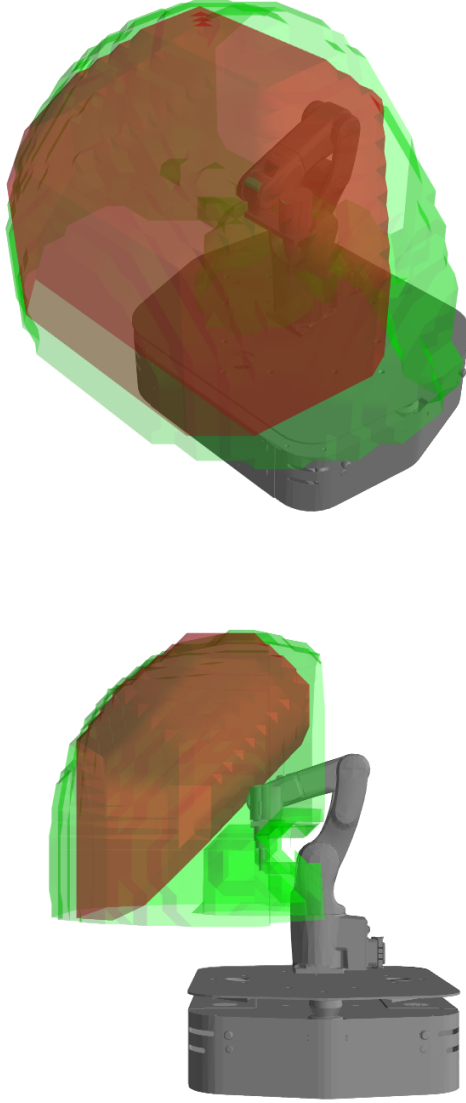


Fig. 3:  $V_{\text{fkr}}$ , shown in green, marks all the voxels on the top-front quarter of the robotic workspace that are reachable from direction  ${}^{\text{base}}\mathbf{R}_{\text{ext}} = \mathbf{R} = [1, 0, 0]$ . The maximal convex subset approximation  $M_{\text{fkr}}$  is shown in red.

of the equilateral triangle  $\triangle efg$ . The solution is provided below as:

$$\delta = \frac{\sqrt{3}}{2}d$$

To obtain  $\mathbf{T}_{\text{base}}^i$ , we match the ball centered at  $\mathbf{c}_i$  with the ball  $\mathcal{B}(\mathbf{c}_i) \subseteq \mathcal{B}$  centered at  $\mathbf{b}_i$ :

$$r = \frac{\text{height}({}^w\mathbf{c}_i) - {}^w b_z^b}{{}^w b_z^t - {}^w b_z^b}$$

$$\mathbf{b}_i = (1 - r) \cdot \mathbf{b}_{\text{bottom}} + r \cdot \mathbf{b}_{\text{top}}$$

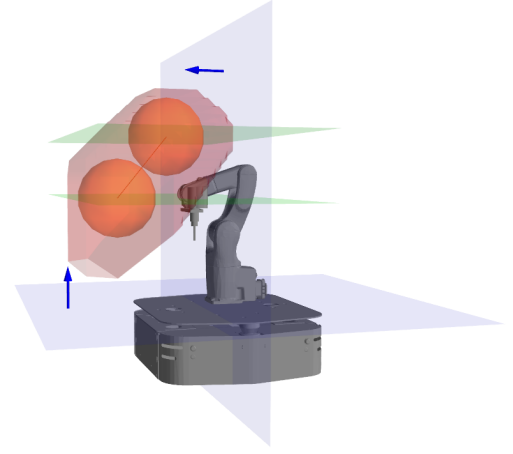


Fig. 4: To find the set  $\mathcal{B}$ , we find the intersection of half-spaces subject to two equality constraints using linear programming. The half-spaces consist of the half-spaces of  $M_{\text{fkr}}$  (red), two collision inequality planes (blue) with vectors showing the normals and two equality planes (green) to cover the minimum and maximum target height respectively. The resulting two balls centered at  $\mathbf{b}_{\text{top}}$  and  $\mathbf{b}_{\text{bottom}}$  are shown in orange. By convexity, any ball centered along the line between the two balls are inside the  $M_{\text{fkr}}$  half-spaces and hence included in the set  $\mathcal{B}$ .

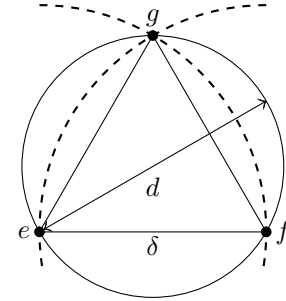


Fig. 5: Diagram containing the minimum circle  $O$  with diameter  $d$  that covers a maximal clique with maximum edge length  $\delta$

satisfying:

$$\begin{aligned} {}^w\mathbf{T}_{\text{base}}^i \cdot {}^{\text{base}}\mathbf{T}_{\mathbf{b}_i} &= {}^w\mathbf{T}_{\mathbf{c}_i} \\ {}^{\text{base}}\mathbf{T}_w \cdot {}^w\mathbf{T}_{\mathbf{c}_i} &= {}^{\text{base}}\mathbf{T}_{\mathbf{b}_i} \\ {}^{\text{base}}\mathbf{T}_{\mathbf{b}_i} &= {}^{\text{base}}\mathbf{T}_{\mathbf{c}_i} \end{aligned}$$

where  $w$  is the world's frame.

The robot's base transformations  ${}^w\mathbf{T}_{\text{base}}^i$  can then be calculated for each  $\mathbf{c}_i$  by simple transformation:

$$\begin{aligned} {}^w\mathbf{T}_{\text{base}}^i &= {}^w\mathbf{T}_{\mathbf{c}_i} \cdot {}^{\mathbf{c}_i}\mathbf{T}_{\text{base}} \\ &= {}^w\mathbf{T}_{\mathbf{c}_i} \cdot ({}^{\text{base}}\mathbf{T}_{\mathbf{c}_i})^{-1} \\ &= {}^w\mathbf{T}_{\mathbf{c}_i} \cdot ({}^{\text{base}}\mathbf{T}_{\mathbf{b}_i})^{-1} \end{aligned}$$

## VI. TASK SEQUENCING

Let  $\text{seq}(g(k))$  be a sequence of  $k$  configurations in the coordinate space spanned by  $g$ . The length of the sequence is defined by  $\text{length}(\text{seq}(g(k))) = \sum_{n=1}^{k-1} \|g(k)_{n+1} - g(k)_n\|$ . When  $g(k)_1 = g(k)_k$ ,  $\text{seq}(g(k))$  forms a tour.

Let  $\mathbf{t} = [t_x, t_y]$  be the base positions. The algorithm consists in:

- 1) Finding a near-optimal base transforms tour  $\text{seq}(\mathbf{t}(c+2))$  in task-space that minimizes  $\text{length}(\text{seq}(\mathbf{t}(c+2)))$ .
- 2) Finding the near-optimal target sequence  $\text{seq}(\mathbf{x}(n+2))$  in task-space given  $\text{seq}(\mathbf{t}(c+2))$ .
- 3) Finding the optimal manipulator  $\mathbf{q}^* = [q_1, \dots, q_{n+2}]$  configuration for each target in  $\text{seq}(\mathbf{x}(n+2))$  such that  $\text{length}(\text{seq}(\mathbf{x}(c+2)))$  is minimum. Collisions are ignored at this stage.
- 4) Computing fast collision-free configuration space trajectories on 9-DOF combined base and manipulator configurations based on  $\text{seq}(\mathbf{t}(c+2))$  and  $\text{seq}(\mathbf{x}(n+2))$ .

Our task sequencing algorithm is inspired by RoboTSP, a fast RTSP solution for fixed-base manipulator [5].

In Step 1, the tour  $\text{seq}(\mathbf{t}(c+2))$  is calculated which starts at predetermined  $\mathbf{t}^{\text{start}}$ , covers all  $\mathbf{t}^i$  for all  $c$  clusters and ends at  $\mathbf{t}^{\text{end}}$  where  $\mathbf{t}^{\text{start}} = \mathbf{t}^{\text{end}}$ . The base station tour is found through finding the approximated solution to the Travelling Salesman Problem (TSP) using the 2-Opt algorithm [20].

In Step 2, the tour  $\text{seq}(\mathbf{x}(n+2))$  is obtained which starts at predetermined  $\mathbf{x}_{\text{start}}$ , covers all  $n$  number of  $\mathbf{x}_i$  and ends at  $\mathbf{x}_{\text{end}}$ . Unlike in previous step, the target tour finding is formulated as a minimum-length Hamiltonian Path problem instead.

This is achieved through virtually translating  $\mathbf{x}_{\text{start}}$ ,  $\mathbf{x}_1$ , ...,  $\mathbf{x}_n$ ,  $\mathbf{x}_{\text{end}}$  along an axis with distance  $h$  between them to form a *stack-of-clusters* as seen in Figure 6. We denote  $\mathbf{x}'$  for the translated  $\mathbf{x}$ . In our implementation, we define  $h$  to be:

$$h = h_{\text{scale}} \cdot \max_{1 \leq i \leq c} \{\text{dist}(a, b) : a, b \in \mathbf{X}_i, a \neq b\}$$

where  $h_{\text{scale}} \geq 1$

The minimum-length Hamiltonian Path is calculated on all targets on the *stack-of-clusters* starting from  $\mathbf{x}'_{\text{start}}$  and ending at  $\mathbf{x}'_{\text{end}}$ . The resulting  $\text{seq}(\mathbf{x}'(n+2))$  is translated back to obtain  $\text{seq}(\mathbf{x}(n+2))$ , which is a target tour sequence that respects the base tour sequence  $\text{seq}(\mathbf{t}(c+2))$  and minimizes manipulator trajectory distance between base movement.

Similar to [5], in Step 3 we firstly construct an undirected graph of  $n+2$  layers following the order in  $\text{seq}(\mathbf{x}(n+2))$ . Each layer  $i$ , where  $i \in [1, n+2]$  contains  $v_i$  nodes representing the number of IK solutions of the 6-DOF manipulator for target  $i$ , resulting in a total of  $\sum_{i=1}^{n+2} v_i$  nodes. Note that the first and last nodes are “Start” and “Goal” nodes respectively such that  $v_1 = v_{n+2} = 1$ . Next for  $i \in [1, n+1]$ , we add an edge between each nodes of layer  $i$  and layer  $i+1$ , resulting in a total of  $\sum_{i=1}^{n+1} v_i v_{i+1}$  edges. Lastly, we find the shortest path between the “Start” and “Goal” nodes using a graph search algorithm to find the optimal sequence of IK solutions.

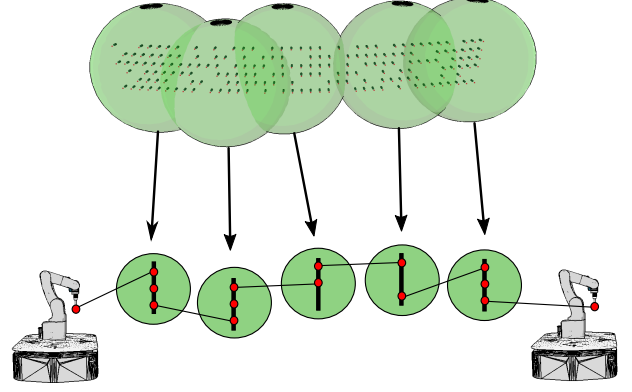


Fig. 6: An illustration of *stack-of-clusters*. The clustered targets (top) are “translated” and stacked *back-to-back* between a Start and End end-effector position to form  $\mathbf{x}'_{\text{start}}$ ,  $\mathbf{x}'_1$ ,  $\mathbf{x}'_2$ ,  $\mathbf{x}'_3$ ,  $\mathbf{x}'_4$ ,  $\mathbf{x}'_5$  and  $\mathbf{x}'_{\text{end}}$  (bottom). Minimum-length Hamiltonian Path is calculated on the “translated” clusters to obtain  $\text{seq}(\mathbf{x}'(7))$ , a target tour that respects the base tour sequence  $\text{seq}(\mathbf{t}(7))$  and minimizes manipulator trajectory distance between base movement.

## VII. EXPERIMENT

For our experiment we generated the fkr dataset for the top-front quarter grid of the robot’s workspace similar to in Figure 3. The distance between two workspace voxels is set at 0.04 m. For  $\mathbf{R}_{\text{ext}}$ , we consider four direction vectors resembling a pyramid that makes  $\theta = 10$  degree from the axis that runs along the pyramid’s height. The four direction vectors are:

- $[\cos(\theta), 0, \sin(\theta)]$
- $[\cos(\theta), 0, -\sin(\theta)]$
- $[\cos(\theta), \sin(\theta), 0]$
- $[\cos(\theta), -\sin(\theta), 0]$

The drill target directions in simulation are then programmed such that they cover the vector range bounded by values in  $\mathbf{R}_{\text{ext}}$ .

Below we provides tables that list the time breakdown of our proposed method. In Table I, we show the time required to perform sampling for  $V_{\text{fkr}}$  and subsequently obtaining the maximal digital convex subset  $M_{\text{fkr}}$ . We consider these as offline processes as they can be pre-generated and reused on other target distributions with similar robot and target directions requirement. Following that, in Table II and Table III we provide the time breakdown for different number of targets for target clustering and target sequencing respectively.

TABLE I: Time breakdown for offline processes

	time (seconds)
$V_{\text{fkr}}$	225.4
$M_{\text{fkr}}$	2516.1



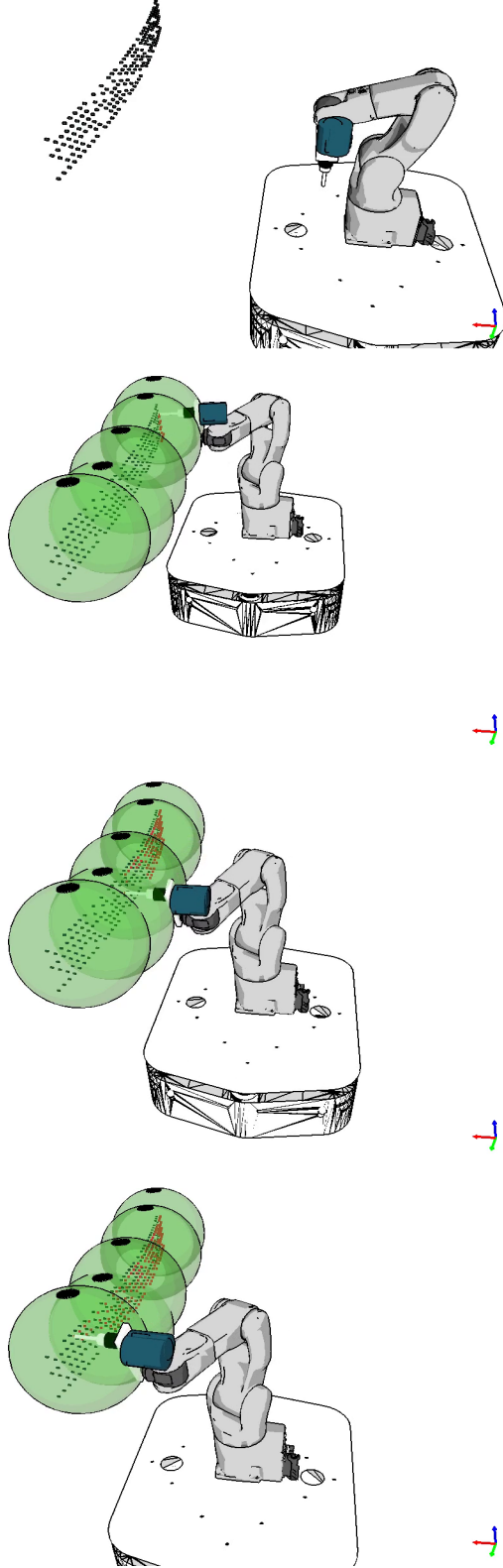


Fig. 7: Simulation in OpenRAVE where the mobile manipulator has to visit 183 non-clustered and unsequenced targets. The algorithm found five *workspace clusters* to visit them. The orientations of the targets cover the range within the bounding directions  $R_{ext}$  used in building the set of  $B$ .

TABLE II: Time breakdown for online target clustering

No of targets	Target clustering in seconds ( $\pm$ std)
183	0.104 ( $\pm$ 0.01)
268	0.209 ( $\pm$ 0.04)
2211	15.887 ( $\pm$ 0.06)

TABLE III: Time breakdown for online target sequencing

No of targets	Base and hole tour finding in seconds ( $\pm$ std)
183	0.919 ( $\pm$ 0.01)
268	3.804 ( $\pm$ 0.06)

## VIII. CONCLUSION

The problem of visiting multiple task points with a mobile manipulator has always been challenging. Compared to its fixed-base counterpart, there are more complexities to deal with when the task space targets span beyond the reachable immediate workspace. Most approaches rely on computationally expensive base poses sampling. To make the problem tractable, they often require the targets to be arbitrarily pre-clustered or pre-sequenced which might not always be possible such as in drilling operations.

In this paper, we introduced a novel approach based on clustering the task point targets first. We presented a fast and principled way to segment the task point targets into reachable clusters, analytically determine base pose for each cluster and find task sequence to minimize robot's trajectory.

The method here can be easily extended to the continuous case, such as in 3D-printing. However, one needs to enforce the continuity of the manipulator motion, which excludes *IK-switching*. Integrating such a constraint into MobaTSP is the objective of our current research.

## ACKNOWLEDGMENT

This research was conducted in collaboration with HP Inc. and supported by National Research Foundation (NRF) Singapore and the Singapore Government through the Industry Alignment Fund-Industry Collaboration Projects Grant (I1801E0028).

## REFERENCES

- [1] S. Vafadar, A. Olabi, and M. S. Panahi, "Optimal motion planning of mobile manipulators with minimum number of platform movements," in *2018 IEEE International Conference on Industrial Technology (ICIT)*, pp. 262–267, IEEE, 2018.
- [2] J. Xu, K. Harada, W. Wan, T. Ueshiba, and Y. Domae, "Planning an efficient and robust base sequence for a mobile manipulator performing multiple pick-and-place tasks," in *2020 IEEE International Conference on Robotics and Automation (ICRA)*, pp. 11018–11024, 2020.
- [3] D. H. Shin, B. S. Hamner, S. Singh, and M. Hwangbo, "Motion planning for a mobile manipulator with imprecise locomotion," in *Proceedings 2003 IEEE/RSJ International Conference on Intelligent Robots and Systems (IROS 2003)(Cat. No. 03CH37453)*, vol. 1, pp. 847–853, IEEE, 2003.
- [4] M. E. Tiryaki, X. Zhang, and Q. Pham, "Printing-while-moving: a new paradigm for large-scale robotic 3d printing," in *2019 IEEE/RSJ International Conference on Intelligent Robots and Systems (IROS)*, pp. 2286–2291, 2019.

- [5] F. Suárez-Ruiz, T. S. Lembono, and Q.-C. Pham, "Robotsp—a fast solution to the robotic task sequencing problem," in *2018 IEEE International Conference on Robotics and Automation (ICRA)*, pp. 1611–1616, IEEE, 2018.
- [6] F. Zacharias, C. Borst, and G. Hirzinger, "Capturing robot workspace structure: representing robot capabilities," in *2007 IEEE/RSJ International Conference on Intelligent Robots and Systems*, pp. 3229–3236, Ieee, 2007.
- [7] F. Zacharias, C. Borst, M. Beetz, and G. Hirzinger, "Positioning mobile manipulators to perform constrained linear trajectories," in *2008 IEEE/RSJ International Conference on Intelligent Robots and Systems*, pp. 2578–2584, IEEE, 2008.
- [8] F. Zacharias, W. Sepp, C. Borst, and G. Hirzinger, "Using a model of the reachable workspace to position mobile manipulators for 3-d trajectories," in *2009 9th IEEE-RAS International Conference on Humanoid Robots*, pp. 55–61, IEEE, 2009.
- [9] N. Vahrenkamp, T. Asfour, G. Metta, G. Sandini, and R. Dillmann, "Manipulability analysis," in *2012 12th IEEE-RAS International Conference on Humanoid Robots (humanoids 2012)*, pp. 568–573, IEEE, 2012.
- [10] N. Vahrenkamp, T. Asfour, and R. Dillmann, "Robot placement based on reachability inversion," in *2013 IEEE International Conference on Robotics and Automation*, pp. 1970–1975, IEEE, 2013.
- [11] P. T. Zacharia and N. Aspragathos, "Optimal robot task scheduling based on genetic algorithms," *Robotics and Computer-Integrated Manufacturing*, vol. 21, no. 1, pp. 67–79, 2005.
- [12] K. Baizid, R. Chellali, A. Yousnadj, A. Meddahi, and T. Bentaleb, "Genetic algorithms based method for time optimization in robotized site," in *2010 IEEE/RSJ International Conference on Intelligent Robots and Systems*, pp. 1359–1364, IEEE, 2010.
- [13] M. Saha, T. Roughgarden, J.-C. Latombe, and G. Sánchez-Ante, "Planning tours of robotic arms among partitioned goals," *The International Journal of Robotics Research*, vol. 25, no. 3, pp. 207–223, 2006.
- [14] G. Borgefors and R. Strand, "An approximation of the maximal inscribed convex set of a digital object," in *International Conference on Image Analysis and Processing*, pp. 438–445, Springer, 2005.
- [15] L. Crombez, G. D. da Fonseca, and Y. Gérard, "Peeling digital potatoes," *arXiv preprint arXiv:1812.05410*, 2018.
- [16] G. B. Dantzig, *Linear programming and extensions*, vol. 48. Princeton university press, 1998.
- [17] A. Kosowski and K. Manuszewski, "Classical coloring of graphs," *Contemporary Mathematics*, vol. 352, pp. 1–20, 2004.
- [18] D. W. Matula and L. L. Beck, "Smallest-last ordering and clustering and graph coloring algorithms," *Journal of the ACM (JACM)*, vol. 30, no. 3, pp. 417–427, 1983.
- [19] N. Deo, J. S. Kowalik, et al., *Discrete optimization algorithms: with Pascal programs*. Courier Corporation, 2006.
- [20] D. L. Applegate, R. E. Bixby, V. Chvatal, and W. J. Cook, *The traveling salesman problem: a computational study*. Princeton university press, 2006.